ACS APPLIED MATERIALS & INTERFACES

Letter

www.acsami.org

Responsive PET Nano/Microfibers via Surface-Initiated Polymerization

A. Evren Özçam,[†] Kristen E. Roskov,[†] Jan Genzer,[†] and Richard J. Spontak*[,†,‡]

[†]Departments of Chemical & Biomolecular Engineering and [‡]Materials Science & Engineering, North Carolina State University, Raleigh, North Carolina 27695, United States

Supporting Information

ABSTRACT: Poly(ethylene terephthalate) (PET) is one of the most important thermoplastics in ubiquitous use today because of its mechanical properties, clarity, solvent resistance, and recyclability. In this work, we functionalize the surface of electrospun PET microfibers by growing poly(*N*-isopropylacrylamide) (PNIPAAm) brushes through a chemical sequence that avoids PET degradation to generate thermoresponsive microfibers that remain mechanically robust. Amidation of deposited 3-aminopropyltriethoxysilane, followed by hydrolysis, yields silanol groups that permit surface attachment of initiator molecules, which can be used to grow PNIPAAm via "grafting from" atom-transfer radical polymerization. Spectroscopic analyses performed after each step confirm the expected reaction and the ultimate growth of PNIPAAm brushes. Water contact-angle measurements conducted at temperatures below and above the lower critical solution temperature of PNIPAAm, coupled with adsorption of Au nanoparticles from aqueous suspension, demonstrate that the brushes retain their reversible thermoresponsive nature, thereby making PNIPAAm-functionalized PET microfibers suitable for filtration media, tissue scaffolds, delivery vehicles, and sensors requiring robust microfibers.

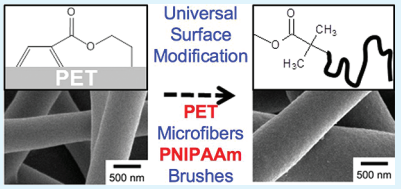

KEYWORDS: *electrospinning, polymer brush, poly(ethylene terephthalate), responsive polymer, surface functionalization*

Electrospinning is an emerging fabrication technique capable of generating solid polymer fibers that range from tens of nanometers to several micrometers in diameter. Such nano/microfibers are of fundamental and technological interest due to their high surface-to-volume ratio. During wet electrospinning, a polymer solution of sufficiently high viscosity and conductivity is subjected to an electric field. When the electrostatic forces overcome surface tension, a charged jet emitted from the tip of a Taylor cone[1] undergoes a whipping action[2] (wherein the solvent evaporates) and is subsequently collected as a dry, randomly oriented fiber mat on a grounded collector plate. This process strategy is appealing due to the simple setup required and the ability to tailor fiber characteristics with relative ease.[3] Although the morphology of electrospun nano/microfibers is desirable, they tend to lack the functionality that is sought in contemporary applications. One way to overcome this deficiency is by developing multicomponent nano/microfibers, in which the fiber-forming polymer is modified with one or more species designed to enhance targeted properties.[4−6] Surface-active compounds added to the polymer solution prior to electrospinning may, however, remain trapped within the resultant fiber upon solidification and thus exhibit substantially reduced activity.[7] While antibacterial biocides incorporated in this fashion lose much of their efficacy,[8] quaternary ammonium species covalently bonded to as-spun fibers can create a permanent antibacterial surface.[9] Alternatively, polarizable antibacterial copolymers codissolved with the fiber-forming polymer can be brought to the fiber surface, where they remain anchored in place, by the electric field during electrospinning.[10,11] Recently, Agarwal et al.[12] have surveyed chemical routes by which to modify and functionalize the surface of electrospun nanofibers for diverse applications ranging from functional textiles, catalyst supports and ion-exchange membranes to drug delivery and tissue engineering.

Polymers such as poly(ethylene terephthalate) (PET), which is widely known for its mechanical strength, transparency and solvent resistance, tend to possess a hydrophobic surface and a low surface energy,[13] in which case electrospun nano/microfibers require post-treatment so that chemically active species are positioned on the fiber surface. Methods by which to achieve such surface functionalization include plasma treatment,[8] mineralization,[14] core−shell formation,[15] chemical vapor deposition[16] or inclusion of reactive compounds.[17,18] Once these chemically active groups are available, covalent bonding,[19] immobilization[20] or electrostatic interactions[21] can be used to introduce functional moieties to the fiber surface without adversely affecting the bulk fiber properties. While surface modification could permit the use of electrospun PET[22] nano/microfibers in filtration media,[23] protective textiles,[24] tissue scaffolds,[25] and drug-delivery vehicles,[26] most of the modification approaches listed above purposefully or inadvertently promote PET degradation. Thus, the conditions by which surface modification is conducted must be monitored carefully to avoid compromising the bulk properties of PET.

Received: November 8, 2011
Accepted: December 27, 2011
Published: January 10, 2012

   dx.doi.org/10.1021/am201559f | *ACS Appl. Mater. Interfaces* 2012, 4, 59−64

Grafting polymer brushes represents an alternative approach by which to modify and control the surface properties of materials.[27] Numerous studies have reported surface-initiated grafting on surfaces of various geometries with a plethora of different monomers by employing numerous polymerization routes. Poly(*N*-isopropylacrylamide) (PNIPAAm) is solely considered here because of its thermoresponsive nature[28] (it possesses a lower critical solution temperature, LCST, in water at ≈32 °C). Prior efforts to polymerize styrene[29,30] and NIPAAm[31,32] on flat PET surfaces have relied on different means of activating the PET surface (e.g., saponification, plasma treatment and aminolysis) for the purpose of attaching initiators. The major drawback of such treatments, however, is that they may seriously deteriorate the mechanical properties of PET and increase its surface roughness by chemical degradation, which would be catastrophic with regard to electrospun PET nano/microfibers due to their fine dimensions. Independent studies[33−35] have confirmed that 3-aminopropyltriethoxysilane (APTES) can be used to functionalize the surface of PET via amidation with negligible degradation. Unlike short alkyl amines (which can diffuse into and react throughout, and thus weaken, PET[36,37]), the bulky triethoxysilane group on APTES hinders diffusion, changes its chemical nature upon amidation and creates a barrier by restricting the diffusion of other APTES molecules. Moreover, since the ethoxysilane groups of APTES are exposed at the polymer/air interface after reaction, hydrolysis of triethoxysilane yields silanol groups that facilitate initiator attachment along the fiber surface.

Thermoresponsive PNIPAAm brushes on electrospun fibers have been recently reported. For instance, Brandl et al.[38] describe the synthesis of a copolymer of 2-hydroxyethyl methacrylate (HEMA) and methyl methacrylate (MMA) and its postpolymerization modification with 2-bromoisobutyryl-bromide to prepare a macroinitiator. They claim that electrospinning of the macroinitiator and subsequent polymerization of NIPAAm results in thermoresponsive polymer brushes. The disadvantage of this technique is that the location of the "active" initiator group in the fiber depends on the dielectrophoretic forces, polarizability contrast and surface tension of the comonomers, which invariably reduces the concentration of "active" initiator centers on the fiber surface. The presence of ester groups between the butyrylbromide group of the initiator and hydroxyethyl group of HEMA likewise yields hydrolytically unstable bonds at pH values greater than 8 and lower than 5. Furthermore, the presence of HEMA comonomer on the macroinitiator may result in swelling and absorption of NIPAAm monomer by the electrospun fiber in the aqueous polymerization medium. Similarly, Fu et al.[39] have synthesized and electrospun a copolymer of 4-vinylbenzylchloride and glycidyl methacrylate. Subsequent modification of the electrospun fibers with sodium azide produces azide surface groups that can be coupled with alkyne-functionalized PNIPAAm chains via a click reaction to generate PNIPAAm surface chains that affect the wettability of the fibers. Such grafting of PNIPAAm brushes on electrospun fibers would be necessarily low because of the sparse population of active azide groups on the fiber surface and the accompanying steric hindrance caused by "grafting to" polymerization.

Despite the myriad of reports regarding fiber preparation via electrospinning, the number of studies on electrospun PET fibers is rather limited.[22,40−47] In this work, we aim to craft a mild and universal way of modifying the surface of electrospun PET fibers to combine the mechanical robustness of PET and the functionality of thermoresponsive PNIPAAm brushes that are covalently attached to the fibers. First, electrospun PET microfibers are modified with APTES to create surface-bound hydroxyl groups for the attachment of [11-(2-bromo-2-methyl)propionyloxy] undecyltrichlorosilane (BMPUS), which serves as an ATRP initiator for the polymerization of NIPAAm. Several analytical techniques are employed to (i) characterize the properties of as-spun and postmodified PET microfibers and (ii) follow the polymerization of NIPAAm via ATRP. In addition, we investigate the thermoresponsive nature of PNIPAAm-decorated PET microfibers by attaching Au nanoparticles at temperatures above and below the LCST of PNIPAAm.

EXPERIMENTAL SECTION

Food-grade recycled PET flakes were kindly supplied by the United Resource Recovery Corp. (Spartanburg, SC). Hexafluoroisopropanol (HFIP) was obtained from Oakwood Products Inc. (Estill, SC), and anhydrous toluene, 2-chlorophenol, APTES, NIPAAm, copper I bromide (CuBr), copper II bromide ($CuBr_2$), and *N*,*N*,*N*′,*N*′,*N*″-pentamethyldiethylenetriamine (PMDETA) were all purchased from Sigma-Aldrich and used as-received. The citrate-stabilized Au nanoparticles[48] (diameter = 16.9 ± 1.8 nm) and BMPUS initiator[49] were prepared as described earlier. The PET flakes were dissolved in HFIP at different concentrations and electrospun at ambient temperature and 10 kV to generate microfibers varying in diameter. Thin films of PET measuring 12 and 180 nm thick, as discerned by ellipsometry (v.i.), were spin-coated at 25 °C on silicon wafers from 0.5 and 3.0 wt % solutions, respectively, in 2-chlorophenol. Microfiber mats and thin films were stored under vacuum for at least 48 h prior to use to remove entrapped solvent.

The APTES was deposited on the PET microfibers and thin films by exposing the samples to 1% (v/v) APTES/anhydrous toluene solutions for 24 h at ambient temperature, followed by sonication in toluene for 10 min to remove loosely adsorbed APTES molecules. The ethoxysilane groups of the surface-anchored APTES molecules were hydrolyzed in acidic water (pH ≈ 4.5−5.0) for 6 h at ambient temperature, and then the fiber mats were washed with copious amount of water. After the samples were dried under reduced pressure, BMPUS was deposited on the PET−BMPUS surfaces by established protocols.[50,51] The PNIPAAm brushes were subsequently grown from PET−SiOH surfaces by ATRP of NIPAAm, as described elsewhere.[48] Briefly, 6.30 g of NIPAAm was dissolved in a mixture of 4.86 g of methanol and 6.30 g of water in an argon-purged Schlenk flask, and oxygen was removed via three freeze−thaw cycles. After removal of oxygen, PMDETA (0.56 g), CuBr (0.16 g), and $CuBr_2$ (0.016 g) were added to the solution prior to an additional freeze−thaw cycle. The Schlenk flask was tightly sealed and transferred to an argon-purged glovebox. Microfiber mats and thin films of PET were submersed in the solution for 8 h at ambient temperature, after which they were removed, promptly rinsed with methanol and deionized water, and then sonicated in deionized water for 10 min. The length of the PNIPAAm brushes can be systematically changed by varying the polymerization time or the rate of polymerization, which is governed by the CuBr/$CuBr_2$ ratio. In the present work, we had no intention of

dx.doi.org/10.1021/am201559f | ACS Appl. Mater. Interfaces 2012, 4, 59−64

investigating different thicknesses of PNIPAAm brushes on electrospun PET fibers.

The thickness of the PET films was measured by variable-angle spectroscopic ellipsometry (J.A. Woollam) at a 70° incidence angle before and after each modification step to discern the PNIPAAm brush height. Surface chemical composition was monitored at each reaction step by X-ray photoelectron spectroscopy (XPS) performed on a Kratos Analytical AXIS ULTRA spectrometer at a single takeoff angle of 90°. Fourier-transform infrared (FTIR) spectroscopic analysis of the PET microfibers was conducted in transmission mode on a Nicolet 6700 spectrometer after embedding the microfiber mats in potassium bromide pellets. For each sample, 1024 scans were acquired after background correction at a resolution of 4 cm^{-1}. Resultant XPS and FTIR spectra were analyzed using the Vision and Omnic Spectra software suites, respectively. The thermoresponsive behavior of PET and PET-PNIPAAm microfibers was interrogated by measuring the static water contact angle (WCA) at different temperatures via the sessile drop technique on a Ramé-Hart Model 100−00 instrument. The WCA measurements performed above ambient temperature were recorded after thermal equilibration in an environmental chamber manufactured by Ramé-Hart. As-spun and modified PET microfibers were coated with ∼8 nm of Au prior to analysis by field-emission scanning electron microscopy (SEM) performed on a JEOL 6400F electron microscope operated at 5 kV. The thickness of the Au layer was sufficiently thick to prevent specimen charging under the electron beam, but sufficiently thin to avoid masking fine features on the surface of the microfibers. The average microfiber diameter and corresponding standard deviation were determined by measuring the diameters of at least 100 microfibers and analyzing the results with the ImageJ software package.

RESULTS AND DISCUSSION

The diameters of electrospun PET microfibers, prepared according to the protocol provided in the Experimental Section and measured by SEM, are 450 ± 100, 800 ± 200, and 1200 ± 300 nm for 6, 8, and 10 wt % solutions, respectively, of PET in HFIP. While the reported average diameters have relatively low standard deviations, microfiber diameters can range from ∼300−3000 nm. The surfaces of unmodified PET microfibers consistently appear smooth (see Figure 1) with some slight dimpling observed occasionally along the fiber axis. Microfibers modified with thermoresponsive PNIPAAm brushes have been generated in a sequence of four steps, which are depicted schematically in Figure 1. Briefly, APTES molecules are attached to the PET surface via aminolysis between PET and the primary amine of APTES. Next, the ethoxysilane groups on APTES are hydrolyzed to generate silanol groups for BMPUS attachment. Finally, PNIPAAm brushes are grown directly from the PET microfiber surface. Utilization of ATRP restricts initiation of PNIPAAm to the PET microfiber surface, thereby eliminating the formation of free PNIPAAm chains in solution. A second SEM image displaying PET microfibers modified with PNIPAAm brushes is included for comparison in Figure 1 to demonstrate that these microfibers appear marginally rougher than the as-spun microfibers at the end of the modification and brush growth process. The difference in microfiber morphology is almost indiscernible, and the PNIPAAm brushes on spin-coated PET films on silicon wafers appear smooth, which together verify that the brush is uniformly distributed on the

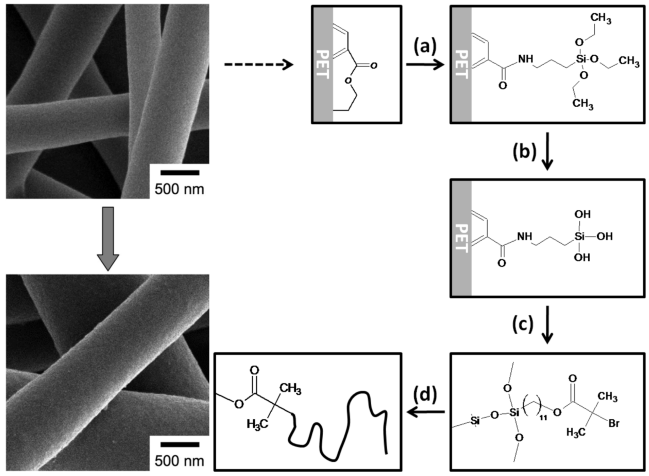

Figure 1. Sequence of surface modification steps employed in this study to functionalize electrospun PET microfibers with thermoresponsive PNIPAAm brushes. The steps require (a) deposition and amidation of APTES, followed by (b) hydrolysis of the ethoxysilane groups on APTES to form silanol groups, which permit (c) attachment of BMPUS and subsequent (d) ATRP of NIPAAm to yield PNIPAAm brushes. The top and bottom SEM images display PET and PET-PNIPAAm microfibers, respectively.

surface of the microfibers. Below, we provide a detailed assessment of each of the steps in this polymerization sequence.

In Figure 2, FTIR spectra are presented for three materials: (a) as-spun microfibers (PET), (b) APTES-modified PET

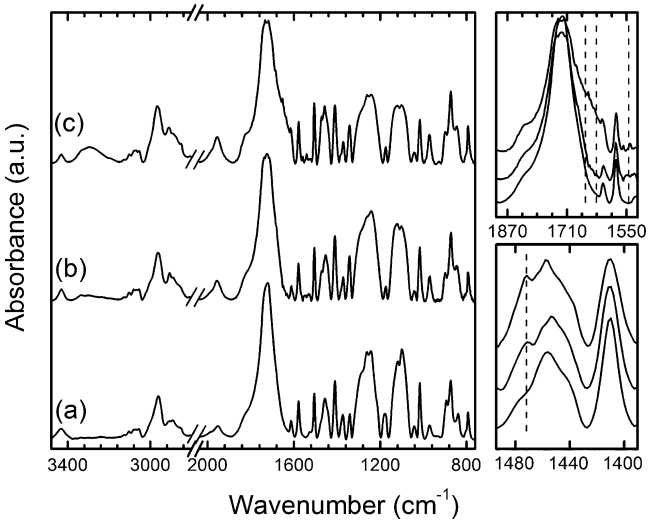

Figure 2. FTIR spectra of (a) as-spun PET, (b) PET-SiOH and (c) PET-PNIPAAm microfibers. Spectra arranged in the same order in the expanded views reveal the appearance of peaks associated with the formation of secondary amide moieties (dotted lines; see text for assignments).

microfibers following hydrolysis (PET-SiOH) and (c) PET microfibers with PNIPAAm brushes (PET-PNIPAAm). The appearance of new peaks located at 1650 cm^{-1} (amide I band), 1550 cm^{-1} (amide II band), 1470 cm^{-1}, and 3300 cm^{-1} in Figure 2b is due to the formation of secondary amide groups, thereby confirming the grafting of APTES to the PET microfiber surface. The formation of silanol groups accompanying hydrolysis of the ethoxysilane groups is also known[52] to contribute to the band located at 3300 cm^{-1}. Previous

dx.doi.org/10.1021/am201559f | ACS Appl. Mater. Interfaces 2012, 4, 59−64

reports[33−35] regarding the surface modification of PET with APTES could not detect the amidation reaction via FTIR due to a very low signal-to-noise ratio. Detection of these groups by FTIR in the present work is attributed to the large surface area afforded by the microfibers. Successful attachment of APTES can also be inferred from the surface properties of modified microfibers upon exposure to acidic water, which promotes hydrolysis of the ethoxysilane groups to silanol groups. Resulting changes in WCA and specimen thickness are measured on flat PET films spin-coated on silicon wafer. Corresponding values of WCA for films of PET-SiOH and PET after hydrolysis are 50 ± 0.8° and 71 ± 0.8°, respectively, whereas that for untreated PET is 75 ± 0.2°. In addition, the XPS results shown in Figure 3a reveal the existence of small

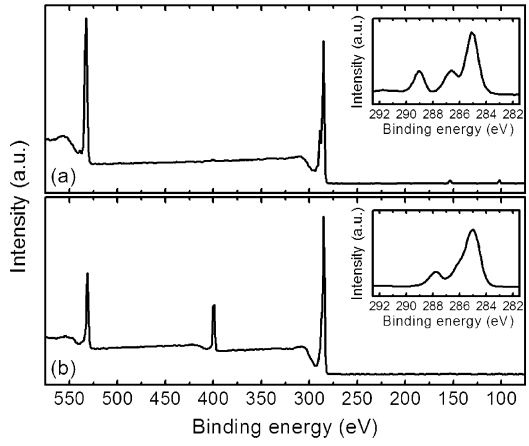

Figure 3. XPS spectra of (a) PET-SiOH microfibers and (b) PET-PNIPAAm microfibers. The survey scans confirm the presence of N upon amidation of PET by APTES in (a) and PNIPAAm brush formation in (b). The high-resolution insets show the C_{1s} peak (~285 eV) before (a) and after (b) PNIPAAm brush growth.

N_{1s}, Si_{2s} and Si_{2p} peaks at 399.7, 153.1, and 101.8 eV, respectively. These peaks correspond to 0.6 atom % N and 1.1 atom % Si from the hydrolyzed APTES on the PET-SiOH surface. In the next step, BMPUS molecules are attached to the PET-SiOH surface (*cf.* Figure 1) to serve as initiator centers for the "grafting from" polymerization of NIPAAm.

Subsequent growth of PNIPAAm brushes from the initiator centers at the fiber surface is verified by the FTIR and XPS spectra presented in Figures 2c and 3b, respectively. The characteristic secondary amide IR vibrations located at 1650, 1550, 1470, and 3300 cm^{-1} are the most pronounced for PET-PNIPAAm microfibers. Moreover, the appearance of a relatively intense N_{1s} peak at 399.7 eV in Figure 3b indicates an elevated concentration of N, which is consistent with the presence of PNIPAAm brushes. Quantitation of this spectrum yields the following atomic concentrations: 76.8 ± 0.4% C, 11.6 ± 0.5% N, and 11.6 ± 0.3% O. These values agree favorably with theoretical concentrations (75.0% C, 12.5% N, and 12.5% O) obtained from the chemical structure of PNIPAAm. The high-resolution C_{1s} spectra included in the insets of Figures 3a and 3b likewise demonstrate that the PNIPAAm brushes cover the PET film surface. In Figure 3a, the spectrum displays peaks at 285.0, 286.6, 289.0, and 291.8 eV corresponding to C−C, C−O, and O−C═O functionalities, as well as "shake up" (the $\pi \rightarrow \pi^*$ transition), respectively. Except for the C−C peak at 285.0 eV, these signature features of PET disappear upon growth of the PNIPAAm brushes, which are responsible for a new peak at 287.8 eV (N−C═O groups) and a shoulder at 286.1 eV (C−N bonds).[53] Additional XPS results are provided in the Supporting Information. Since the XPS fingerprint for PET is lost upon PNIPAAm brush growth, it can be inferred that the thickness of the dry brushes is at least comparable to the probe depth of XPS (~10 nm). According to ellipsometry measurements of PET−PNIPAAm films on silicon wafer, the dry thickness of the PNIPAAm brush after a polymerization time of 8 h is ~40 nm, which, assuming an average grafting density of 0.45 chains/nm^2, corresponds to a molecular weight of ~48 kDa.[54,55] Although the microfibers possess a curved surface, we contend that, on the basis of the brush gyration diameter (~40 nm) relative to the average microfiber diameter (450−1200 nm), the thickness of the PNIPAAm brush does not differ substantially from that produced on a flat film.

The thermoresponsiveness of the PNIPAAm brushes grown on PET microfibers is first evaluated with WCA experiments performed successively above and below the LCST of PNIPAAm, as shown in Figure 4. The WCA of unmodified

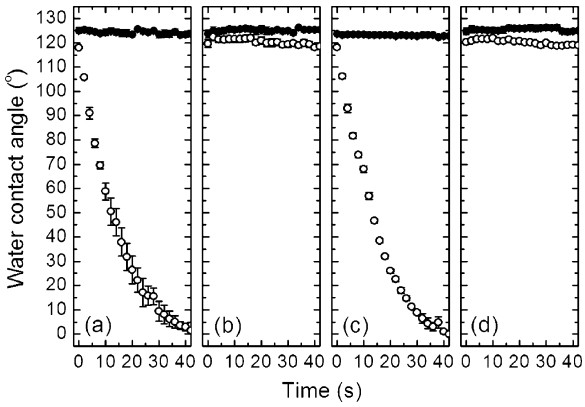

Figure 4. WCA measurements of as-spun PET (●) and PET-PNIPAAm (○) microfibers exposed in cyclic fashion to temperatures (in °C) below and above the LCST of PNIPAAm: (a) 25, (b) 60, (c) 25, and (d) 60. The error bars correspond to the standard deviation of the data.

PET microfibers at 25 °C (Figure 4a) is ~125°, which is higher than that of a flat PET film (75°) because of the "rough" nature of the microfiber mat. Despite this increase in surface roughness, the size of the water droplet on the surface of unmodified PET microfibers does not change during the course of the measurement, and the measured WCA remains constant. This result also verifies that no significant evaporation of water takes place during the course of the WCA measurement because liquid evaporation during WCA measurement may sometimes reduce the apparent contact angle values due to pinning of the contact line. In Figure 4b, the WCA of the unmodified PET microfibers at 60 °C is ~124° and likewise does not change, which suggests that water evaporation is negligible. Cycling the specimen between these two temperatures in Figures 4c and 4d yields comparable results, confirming that the PET surface stays hydrophobic. Measured WCA values of PET-PNIPAAm microfibers, on the other hand, display significantly different behavior. At 25 °C (Figure 4a), the WCA is also ≈125° when the water droplet is initially placed on the microfiber surface, but quickly decreases to 0° in just over 40 s as the water is wicked by the hydrophilic PNIPAAm brushes on the surface of the microfibers. When the

dx.doi.org/10.1021/am201559f | *ACS Appl. Mater. Interfaces* 2012, 4, 59−64

temperature is increased above the LCST of PNIPAAm to 60 °C (Figure 4b), the water droplet is not strongly affected by the microfiber due to the increased hydrophobicity of the PNIPAAm chains, and the WCA remains ~124°. Repetition of these measurements upon thermal cycling in Figures 4c and 4d confirms that the thermoresponsiveness of PNIPAAm brushes on PET microfibers is reversible with no evidence of hysteresis.

A second probe of the thermoresponsive nature of PNIPAAm brushes on PET microfibers employs Au nanoparticles as tracers. Previous studies[48,56] have established that Au nanoparticles attach to PNIPAAm chains via hydrogen bonding between the citrate groups present on the nanoparticle surface and the amide groups on PNIPAAm. To discern whether the PNIPAAm brushes grown on PET microfibers bind Au nanoparticles, modified microfibers have been submerged in a 0.05 mg/mL suspension of Au nanoparticles in deionized water for 24 h at the same two temperatures examined in Figure 4, namely, 25 and 60 °C. Images acquired by SEM reveal that the nanoparticle loading on the surface of dried PET-PNIPAAm microfibers is significantly higher at 25 °C (Figure 5a) than at 60 °C (Figure 5b). This difference is attributed to the thermoresponsiveness of the PNIPAAm chains, which are hydrophilic and swell in water at temperatures below the LCST, but become hydrophobic and collapse in water at temperatures above the LCST. As a result of such temperature-driven swelling or contracting of the brush, the number of NIPAAm units available for Au attachment increases or decreases, respectively, which, in turn, governs the concentration of Au nanoparticles bound to PNIPAAm. Complementary UV spectra confirming the presence of Au nanoparticles attached to the PET-PNIPAAm microfibers at 25 °C are provided in the Supporting Information.

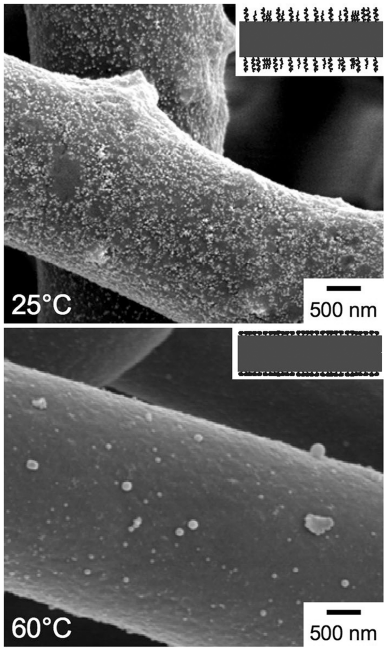

Figure 5. SEM images acquired from PET-PNIPAAm microfibers exposed to aqueous suspensions of Au nanoparticles at temperatures (labeled) below and above the LCST of PNIPAAm. The illustrations in the insets (not drawn to scale) portray the conformation of the PNIPAAm brush at each temperature.

CONCLUSIONS

In this study, we have demonstrated that the surface of electrospun PET microfibers can be modified via amidation of the amine group on APTES with the ester group on PET to permit further chemical modification ultimately resulting in the growth of polymer brushes by ATRP. Step-by-step examination of the PET surface during the modification sequence, along with quantitative analysis whenever possible, verifies the expected reaction outcome, and establishes the sequence as a straightforward and viable route for PET microfiber functionalization. The thermoresponsive behavior of the PNIPAAm brushes on PET microfibers has been investigated using both contact-angle measurements to determine the nature of the modified PET surface and Au nanoparticle tracers to establish that brush swelling(collapse) occurs at temperatures below-(above) the LCST of PNIPAAm in water. Surface functionalization of electrospun PET microfibers using this approach and PNIPAAm in particular yields mechanically robust and highly porous mats that are temperature-sensitive, which means that they are suitable candidates for contemporary technologies such as responsive filters, scaffolds, delivery vehicles, and sensors.

ASSOCIATED CONTENT

Supporting Information

Additonal experimental detail, figures showing high-resolution XPS and UV−vis spectra, and a table listing the surface compositions of PET microfibers. This material is available free of charge via the Internet at http://pubs.acs.org.

AUTHOR INFORMATION

Corresponding Author

*E-mail: Rich_Spontak@ncsu.edu.

ACKNOWLEDGMENTS

This work was supported by the United Resource Recovery Corporation and the National Science Foundation through a Graduate Fellowship (K.E.R.).

REFERENCES

(1) Taylor, G. *Proc. Royal Soc. A (London)* **1969**, *313*, 453.
(2) Shin, Y. M.; Hohman, M. M.; Brenner, M. P.; Rutledge, G. C. *Appl. Phys. Lett.* **2001**, *78*, 1149.
(3) Fridrikh, S. V.; Yu, J. H.; Brenner, M. P.; Rutledge, G. C. *Phys. Rev. Lett.* **2003**, 90.
(4) Chae, S. K.; Park, H.; Yoon, J.; Lee, C. H.; Ahn, D. J.; Kim, J. M. *Adv. Mater.* **2007**, *19*, 521.
(5) Son, W. K.; Youk, J. H.; Lee, T. S.; Park, W. H. *Macromol. Rapid Commun.* **2004**, *25*, 1632.
(6) Dzenis, Y. *Science* **2004**, *304*, 1917.
(7) Sundarrajan, S.; Ramakrishna, S. *J. Mater. Sci.* **2007**, *42*, 8400.
(8) Yao, C.; Li, X. S.; Neoh, K. G.; Shi, Z. L.; Kang, E. T. *Appl. Surf. Sci.* **2009**, *255*, 3854.
(9) Lin, J.; Qiu, S. Y.; Lewis, K.; Klibanov, A. M. *Biotechnol. Bioeng.* **2003**, *83*, 168.
(10) Sun, X. Y.; Shankar, R.; Börner, H. G.; Ghosh, T. K.; Spontak, R. J. *Adv. Mater.* **2007**, *19*, 87.
(11) Sun, X. Y.; Nobles, L. R.; Börner, H. G.; Spontak, R. J. *Macromol. Rapid Commun.* **2008**, *29*, 1455.
(12) Agarwal, S.; Wendorff, J. H.; Greiner, A. *Macromol. Rapid Commun.* **2010**, *31*, 1317.
(13) Dann, J. R. *J. Colloid Interface Sci.* **1970**, *32*, 302.
(14) Chen, J. L.; Chu, B.; Hsiao, B. S. *J. Biomed. Mater. Res. A* **2006**, *79A*, 307.

(15) Muller, K.; Quinn, J. F.; Johnston, A. P. R; Becker, M.; Greiner, A.; Caruso, F. *Chem. Mater.* **2006**, *18*, 2397.
(16) Ho, C. C.; Chen, W. S.; Shie, T. Y.; Lin, J. N.; Kuo, C. *Langmuir* **2008**, *24*, 5663.
(17) Luong, N. D.; Moon, I. S.; Lee, D. S.; Lee, Y. K.; Nam, J. D. *Mater. Sci. Eng., C* **2008**, *28*, 1242.
(18) Dong, F. X.; Li, Z. Y.; Huang, H. M.; Yang, F.; Zheng, W.; Wang, C. *Mater. Lett.* **2007**, *61*, 2556.
(19) Ye, P.; Xu, Z. K.; Wu, J.; Innocent, C.; Seta, P. *Biomaterials* **2006**, *27*, 4169.
(20) Wang, Z. G.; Wan, L. S.; Xu, Z. K. *Soft Matter* **2009**, *5*, 4161.
(21) Wang, X. Y.; Kim, Y. G.; Drew, C.; Ku, B. C.; Kumar, J.; Samuelson, L. A. *Nano Lett.* **2004**, *4*, 331.
(22) Chronakis, I. S.; Milosevic, B.; Frenot, A.; Ye, L. *Macromolecules* **2006**, *39*, 357.
(23) Kaur, S.; Ma, Z.; Gopal, R.; Singh, G.; Ramakrishna, S.; Matsuura, T. *Langmuir* **2007**, *23*, 13085.
(24) Lee, S.; Obendorf, S. K. *Text. Res. J.* **2007**, *77*, 696.
(25) Liao, S.; Murugan, R.; Chan, C. K.; Ramakrishna, S. *J. Mech. Behav. Biomed. Mater.* **2008**, *1*, 252.
(26) Zeng, J.; Aigner, A.; Czubayko, F.; Kissel, T.; Wendorff, J. H.; Greiner, A. *Biomacromolecules* **2005**, *6*, 1484.
(27) Bhat, R. R.; Tomlinson, M. R.; Wu, T.; Genzer, J. In *Surface-Initiated Polymerization II*; Springer-Verlag: Berlin, 2006; p 51.
(28) Kidoaki, S.; Ohya, S.; Nakayama, Y.; Matsuda, T. *Langmuir* **2001**, *17*, 2402.
(29) Roux, S.; Demoustier-Champagne, S. *J. Polym. Sci. A: Polym. Chem.* **2003**, *41*, 1347.
(30) Bech, L.; Elzein, T.; Meylheuc, T.; Ponche, A.; Brogly, M.; Lepoittevin, B.; Roger, P. *Eur. Polym. J.* **2009**, *45*, 246.
(31) Farhan, T.; Huck, W. T. S. *Eur. Polym. J.* **2004**, *40*, 1599.
(32) Alem, H.; Duwez, A. S.; Lussis, P.; Lipnik, P.; Jonas, A. M.; Demoustier-Champagne, S. *J. Membr. Sci.* **2008**, *308*, 75.
(33) Fadeev, A. Y.; McCarthy, T. J. *Langmuir* **1998**, *14*, 5586.
(34) Bui, L. N.; Thompson, M.; McKeown, N. B.; Romaschin, A. D.; Kalman, P. G. *Analyst* **1993**, *118*, 463.
(35) Xiang, J. H.; Zhu, P. X.; Masuda, Y.; Koumoto, K. *Langmuir* **2004**, *20*, 3278.
(36) Ellison, M. S.; Fisher, L. D.; Alger, K. W.; Zeronian, S. H. *J. Appl. Polym. Sci.* **1982**, *27*, 247.
(37) Avny, Y.; Rebenfeld, L. *J. Appl. Polym. Sci.* **1986**, *32*, 4009.
(38) Brandl, C.; Greiner, A.; Agarwal, S. *Macromol. Mater. Eng.* **2011**, *296*, 858.
(39) Fu, G. D.; Xu, L. Q.; Yao, F.; Zhang, K.; Wang, X. F.; Zhu, M. F.; Nie, S. Z. *ACS Appl. Mater. Interfaces* **2009**, *1*, 239.
(40) Ma, Z. W.; Kotaki, M.; Yong, T.; He, W.; Ramakrishna, S. *Biomaterials* **2005**, *26*, 2527.
(41) Mazinani, S.; Ajji, A.; Dubois, C. *J. Polym. Sci. B: Polym. Phys.* **2010**, *48*, 2052.
(42) Chen, H.; Liu, Z.; Cebe, P. *Polymer* **2009**, *50*, 872.
(43) Chronakis, I. S.; Jakob, A.; Hagstrom, B.; Ye, L. *Langmuir* **2006**, *22*, 8960.
(44) Hong, K. H.; Kang, T. J. *J. Appl. Polym. Sci.* **2006**, *100*, 167.
(45) Ignatova, M.; Yovcheva, T.; Viraneva, A.; Mekishev, G.; Manolova, N.; Rashkov, I. *Eur. Polym. J.* **2008**, *44*, 1962.
(46) Veleirinho, B.; Rei, M. F.; Lopes-da-Silva, J. A. *J. Polym. Sci. B: Polym. Phys.* **2008**, *46*, 460.
(47) Jung, K. H.; Huh, M. W.; Meng, W.; Yuan, J.; Hyun, S. H.; Bae, J. S.; Hudson, S. M.; Kang, I. K. *J. Appl. Polym. Sci.* **2007**, *105*, 2816.
(48) Bhat, R. R.; Genzer, J. *Appl. Surf. Sci.* **2006**, *252*, 2549.
(49) Matyjaszewski, K.; Miller, P. J.; Shukla, N.; Immaraporn, B.; Gelman, A.; Luokala, B. B.; Siclovan, T. M.; Kickelbick, G.; Vallant, T.; Hoffmann, H.; Pakula, T. *Macromolecules* **1999**, *32*, 8716.
(50) Tomlinson, M. R.; Efimenko, K.; Genzer, J. *Macromolecules* **2006**, *39*, 9049.
(51) Bhat, R. R.; Tomlinson, M. R.; Genzer, J. *Macromol. Rapid Commun.* **2004**, *25*, 270.
(52) Socrates, G. *Infrared and Raman Characteristic Group Frequencies: Tables and Charts*, 3rd ed.; Wiley: Chichester, U.K., 2004.
(53) Beamson, G.; Briggs, D. J. *High Resolution XPS of Organic Polymers: The Scienta ESCA300 Database*; Wiley: Chichester, England, 1992.
(54) Tomlinson, M. R.; Genzer, J. *Langmuir* **2005**, *21*, 11552.
(55) Tomlinson, M. R.; Genzer, J. *Polymer* **2008**, *49*, 4837.
(56) Gupta, S.; Agrawal, M.; Uhlmann, P.; Simon, F.; Stamm, M. *Chem. Mater.* **2010**, *22*, 504.